Journal of Applied Polymer Science

Morphological and mechanical behavior of chemically treated jute-PHBV bio-nanocomposites reinforced with silane grafted halloysite nanotubes

Shaik Zainuddin,[1] Abdullah Fahim,[1] Shaik Shoieb,[2] Farooq Syed,[1] Mahesh V. Hosur,[1] Dawen Li,[2] Chelsea Hicks,[1] Shaik Jeelani[1]

[1]Department of Materials Science and Engineering, Tuskegee University, Tuskegee, Alabama 36088

[2]Department of Electrical Engineering, University of Alabama, Tuscaloosa, Alabama 35487

Correspondence to: S. Zainuddin (E-mail: szainuddin@mytu.tuskegee.edu)

ABSTRACT: In this study, at first, thin films of poly(3-hydroxybutyrate-*co*−3-hydroxyvalerate) (PHBV) nanocomposites were prepared by adding 1–3 wt % grafted halloysite nanotubes (G-HNTs). Jute-PHBV bio-nanocomposites were then fabricated using these films and chemically treated jute fibers in a compression mold machine. The effect of treatment and modification on jute fiber and halloysite nanotubes (HNTs), and the change in their morphology was investigated using Fourier transform infrared (FTIR) spectroscopy, X-ray diffraction (XRD), scanning and transmission electron microscopy (SEM, TEM). Flexural and thermomechanical properties were determined using a three-point bend test and dynamic mechanical analysis (DMA). The results showed separation of fiber bundles with rough fiber surfaces, and grafting of silane coupling agents on fibers and HNTs after the chemical treatment. As a result, a strong bonding was established between the PHBV, G-HNTs and jute fibers that lead to significant improvements in flexural and thermomechanical properties of jute-PHBV bio-nanocomposites. © 2016 Wiley Periodicals, Inc. J. Appl. Polym. Sci. **2016**, *133*, 43994.

KEYWORDS: biomaterials; grafting; mechanical properties; morphology; nanoparticles

Received 1 November 2015; accepted 25 May 2016
DOI: 10.1002/app.43994

INTRODUCTION

Researchers and many government agencies are looking for alternate materials that are efficient, environmentally friendly and inexpensive to replace traditional synthetic polymeric materials. In recent years, materials extracted from natural resources such as biopolymers and natural fibers have shown considerable potential in automotive, food packaging and medical field industries.[1–5] These materials are inexpensive, recyclable, biodegradable, non-toxic and environmentally friendly.[1,6,7] However, there are some difficulties that have prevented the extended utilization of these materials. The most commonly preferred natural fiber, that is, jute fiber is inexpensive, commercially available in the required form and has higher strength and modulus than plastic.[8]

The main elements of jute fibers are cellulose, hemicelluloses, lignin, and pectin. Cellulose is resistant to alkali but hydrolyzes in acid. Hemicellulose is hydrophilic, soluble in alkali, and hydrolyze in acids easily. Lignin is amorphous and hydrophobic in nature that has aromatic and aliphatic constituents in its structure. On the contrary, pectins are waxy elements that provide plant flexibility. The presence of hydroxyl (—OH) groups in jute fibers, like other ligonocellulosic fibers, makes them susceptible to moisture, and hence directly impairs the properties of jute composites, especially dimensional stability. Also, natural fibers do not efficiently adhere to non-polar matrices due to this polar group which leads to weak load transfer from matrix to fiber resulting in poor mechanical properties. To reduce the hydrophilic nature of jute fibers and improve the adhesion properties, it is necessary to modify the surface.[9] Several methods have been used to modify natural fiber surfaces, such as alkali treatment,[10,11] pre-impregnation of fibers,[12] maleic anhydride as copolymers[13,14] and silane grafting.[7,15–17] Van de Weyenburg *et al.*[18] reported up to 30% increase in the tensile strength and modulus of flax/epoxy composites after alkali treatment. Zini *et al.*[19] found that surface acetylation of the flax fiber promotes fiber-matrix interaction and improved the mechanical properties of flax/PHBV composites. Silane treatment was also carried out by immersing the fibers in a weak solution of a silane diluted in a water/alcohol or water/ketone mixture. In the presence of water, silane breaks down into silanol and alcohol. Thus, the silanol reacts with the OH groups of cellulose in natural fibers, forming stable covalent bonds on the cell walls that are chemisorbed onto the fiber surface.[20] The

degree of crosslinking in the interface region and a stronger bonding between fiber and matrix due to increase in fiber surface area after silane treatment was found.[21] Recently, researchers have used a combination of alkali and silane treatments on natural fibers. Herrera-Franco *et al.*[15] and Huda *et al.*[21] performed alkali and silane treatments either in isolation and combination on henequen and flax fibers and investigated their tensile and flexure properties by reinforcing with different polymers. They reported optimum improvement in these properties in an alkali and silane treated fiber composites.

On the contrary, biopolymers such as bionolle, poly(3-hydroxybutyrate-*co*−3-hydroxyvalerate) (PHBV) and polylactic acid (PLA)[19] are used with natural fiber reinforced composites. Among these polymers, PHBV can be considered as true biopolymer as they are synthesized by bacteria as macromolecules. However, the PHBV thermoplastic polymer has relatively lower mechanical properties and poor thermal stability in comparison with synthetic polymers which restricts their use in many applications.

In recent years, HNTs, a member of Kaolin group has attracted the interest as a reinforcement material due to its tube like structure similar to carbon nanotubes with diameters typically smaller than 100 nm and length in between 500 nm to 1.2 microns.[22] The external surface of HNTs is mainly composed of the siloxane (Si—O—Si) groups, whereas the internal surface consists of a gibbsite like array of aluminol (Al—OH) groups.[23] HNTs contain two types of hydroxyl groups, which are situated on the surface of nanotubes and in between the layers which are called inner and outer hydroxyl groups, respectively. The presence of hydroxyl groups that form hydrogen bonding with the polymer matrix favors good dispersion.[24,25] Incorporation of HNTs in various polymers is reported to significantly improve the tensile strength and stiffness, thermal stability, fire retardency and moisture resistance.[26–28]

However, to the best of our knowledge, no study is reported on 100% jute-PHBV bio-nanocomposites by adding the promising grafted natural HNTs. We strongly believe that grafting of HNTs and jute fibers with strong nucleophile amino functional groups will establish a three-way reaction with the carbonyl groups of PHBV polymer forming stable covalent bonds, and may improve the overall performance of these composites significantly. We focused on investigating the effect of alkali and silane treatment of jute fibers, and the addition of grafted HNTs (G-HNTs) on the morphology of PHBV polymer and, flexural and thermomechanical properties of jute-PHBV bio-nanocomposites in this study.

EXPERIMENTAL

Materials

The bacterial grade Poly (3-hydroxybutyrate-*co*−3-hydroxyvalerate) (PHBV), containing 12 mol % of valerite was supplied by Goodfellow Cambridge Limited, UK. This material is an easily melt processible semicrystalline thermoplastic polyester available in pellet form made by biological fermentation. An unmodified tubular shaped halloysite nanotubes (HNTs) was obtained from Natural Nano, Inc. The measured pore volume of HNT is 0.17–0.19cc/g. Woven jute fabric (Natural Color Burlap, Width 47″, weight-11 Oz, Product ID# BURNATU) with an average fiber thickness of 0.5 mm was supplied by OnlineFabricStore.net. Silane coupling agent, 3-aminopropyl triethoxy silane (APTES) was used as a coupling agent for surface modification of jute fiber and HNTs. Ethanol (CH_3CH_2OH) and acetic acid (CH_3COOH) were used for the treatment. All of these chemicals were bought from Sigma Aldrich Inc.

Processing

Grafting of HNTs. A mixture of ethanol and water in a ratio of 80:20 was taken in a glass beaker. A total of 10 mL of silane was then added into the mixture and stirred for 5 min. The pH of the total solution was kept at 4.0 by adding acetic acid to the mixture, as silane is more stable in slightly acidic condition. A total of 50 g of unmodified HNTs was then added into the solution and stirred well using a magnetic stirrer bar and plate. The solution was then dried at room temperature to evaporate ethanol and water, followed by vacuum drying in oven for 24 hr. Finally, dried particles were grinded using a mortar and filtered with 10 μ sieve to obtain finer G-HNTs.

Alkali Treatment and Silane Grafting of Jute Fibers. Jute fibers were first alkali treated with a solution of NaOH to remove lignin, hemi-cellulose and pectin from the fiber. Jute fibers were weighed before the treatment and kept in a solution of 5% NaOH at 23 °C for 2 h. A ratio of 1:20 between the fiber and NaOH solution was maintained for this treatment. Subsequently, the fibers were washed thoroughly with distilled water. A total of 2% acetic acid solution was then added to the alkali treated fiber in order to neutralize the solution followed by continuous washing of fibers using distilled water until the pH reaches to 7.0. Fibers were then dried in an oven kept at 120 °C to remove the moisture. For silane grafting, 2 wt % APTES was added in 80:20 ethanol/water solution. The pH of the solution was kept at 4.0 using acetic acid. Alkali treated jute fibers were then dipped into this solution and kept for 1 h. Finally, the fibers were washed with distilled water and dried in an oven at 120 °C to remove the water and ethanol present in the fibers.

Fabrication of PHBV/G-HNTS Bio-Nanocomposite Film and Jute-PHBV Bio-Nanocomposites

Before processing, PHBV pellets and G-HNTs were dried well at 70 °C for 12 h to remove the moisture content in order to avoid possible polymer degradation. A total of 1–3 wt % G-HNTs were premixed with PHBV pellets before melt mixing. PHBV bio-nanocomposites with 1–3 wt % G-HNTs concentration were then prepared using a single screw extruder machine. The extruder was operated at 100 rpm and the temperature of different zones was kept in the range of 145–166 °C to avoid degradation of polymer and fillers. Samples collected from the extruder machine were then compression molded using a Wabash hot press to get nanocomposite films of thickness 0.45–0.48 mm. During compression molding, a 2.5 ton force was applied for 10 min on the set-up and the temperature was maintained at 166 °C. Neat PHBV composite films were also prepared using the same procedure for baseline comparison.

For jute-PHBV bio-nanocomposites, the fibers and films were stacked in alternate layers and placed in between the two hot

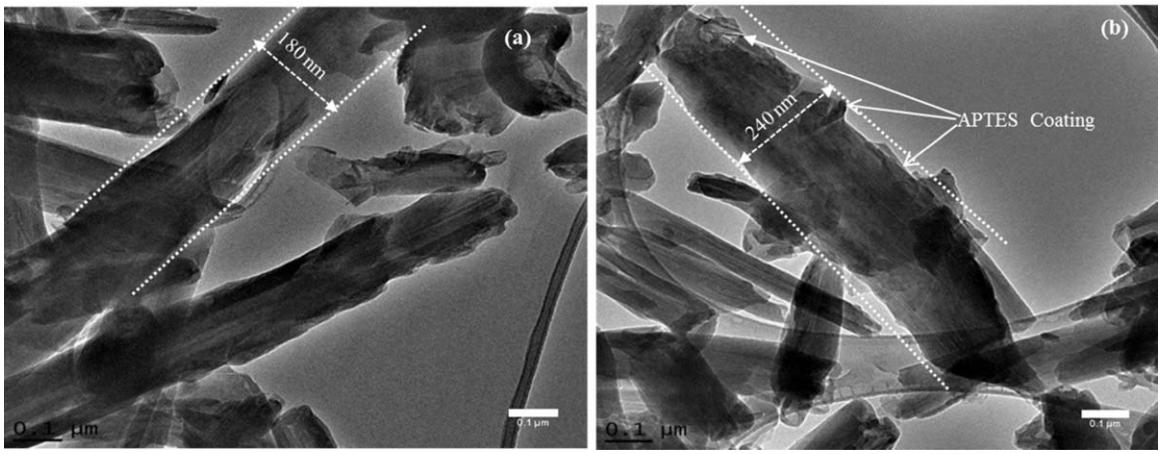

Figure 1. TEM images of (a) unmodified HNTs and (b) G-HNTs.

plates of a compression mold machine. The panels were prepared by compressing the fiber-film arrangement using 1.5 tons of force for 15 min at a temperature of 166 °C and finally cooled to room temperature.

CHARACTERIZATION METHODS

Micrographic Analysis

Transmission electron microscopy (TEM) was carried out at 60 kV using JOEL 2010 to investigate the morphology of pure and grafted HNTs. At first, a drop of colloidal solution containing the HNTs dispersed in ethanol was placed on a copper grid. The grid was then inserted into the TEM chamber for analysis. JEOL JSM-6400 scanning electron microscopy (SEM) was used to study the morphology of untreated (UT), alkali treated (AT), and alkali and silane treated (AST) jute-fibers, as well to analyze the fractured surfaces of these specimens after flexure tests. The surfaces of fibers and fractured specimens were gold sputtered to increase the conductivity. An accelerating voltage of 5 kV was maintained in the SEM.

Fourier Transform Infrared (FTIR) Spectroscopy

Structural characterization of HNTs and jute fibers were performed using a Shimadzu FTIR 8400s instrument equipped with MIRacleTM ATR. The samples were scanned from 550–3500 cm − 1 with a resolution of 4 cm^{-1}.

X-ray Diffraction (XRD) Analysis

XRD patterns of G-HNTS powder, PHBV, and PHBV/G-HNTs samples with different HNT loadings were recorded by Rigaku D/MAX 2200 X-ray diffractometer with Cu Kα radiation ($\lambda = 1.54$ Å) min and operating at 40 kV and 30 mA with a scanning speed of 3° per minute. During the XRD experiments, the samples were analyzed in the reflection mode.

Flexure Test and Dynamical Mechanical Analysis (DMA)

Three-point bend flexure test was performed on UT, AT, and AST samples according to ASTM D790-10 on a Zwick-Roell test machine. At least five samples of each set with dimensions 92 × 12 × 4.5 mm were tested at a crosshead speed of 2 mm/min, while maintaining a span-to-length ratio of 16:1.

DMA was also performed on these samples according to ASTM D4065-01 on a TA instrument Q 800. Samples of size 60 × 12.5 × 4.5 mm were loaded in a double cantilever beam mode. A frequency of 15 Hz, an amplitude of 15 μm and a temperature ramp rate of 5 °C/min was used. At least three samples of each set were tested, and an average was taken to get the storage modulus, loss modulus and tan delta, respectively.

RESULTS AND DISCUSSION

TEM and FTIR Analysis of HNTs

Figure 1 shows the TEM images of both unmodified and G-HNTs. It was found that after the silane treatment, the outer diameter of G-HNTs increased by 60 nm in comparison with unmodified HNTs determined using the ImageJ software. To confirm that the increase in diameter of G-HNTs is due to successful grafting of silane coupling agents on its surface, FTIR analysis was carried out that showed several additional peaks in G-HNTs in contrast to unmodified HNTs (Figure 2). The observed new bands were C—H symmetric and asymmetric vibration band around 2966 and 2876 cm^{-1}, and the deformation C—H vibration band at 1468 cm^{-1}.[22] Also, the N—H deformation vibration band at 1550 cm^{-1} [29] is resulted due to the N—H group strongly bonded with hydroxyl groups of both HNTs and silanol group. Also, N-H asymmetric stretching at

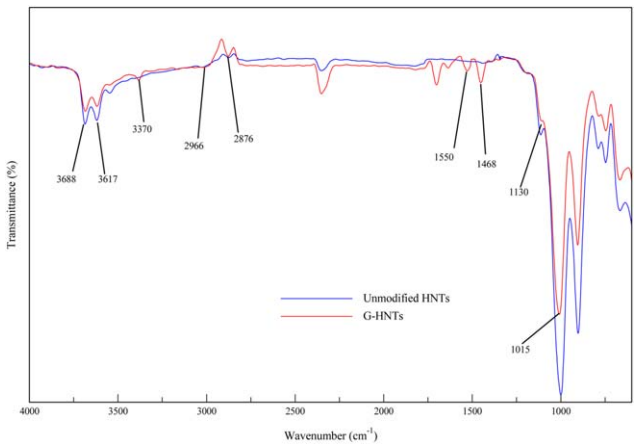

Figure 2. FTIR spectra of unmodified HNTs and G-HNTs. [Color figure can be viewed in the online issue, which is available at wileyonlinelibrary.com.]

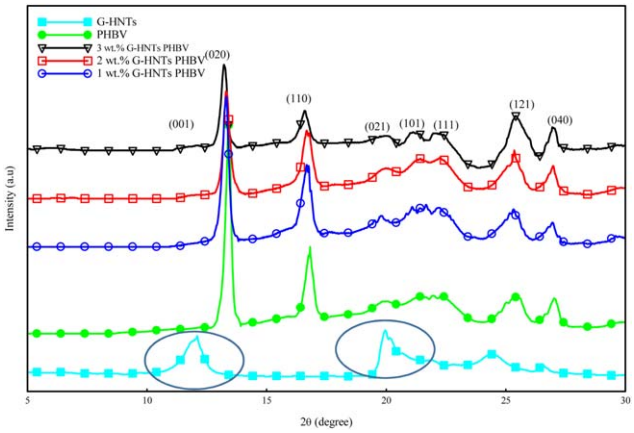

Figure 3. XRD pattern of pure HNTs, PHBV, and G-HNTs added PHBV bio-nanocomposites. [Color figure can be viewed in the online issue, which is available at wileyonlinelibrary.com.]

3370 cm^{-1} indicated the presence of unreacted NH_2 group in G-HNTs samples. Furthermore, the unmodified HNTs showed spectra at 3617 and 3688 cm^{-1} [29] which is due to the presence of surface hydroxyl groups. However, in G-HNTs, the intensity of these bands decreased considerably indicating that the modification was accompanied by the consumption of surface hydroxyl groups. Moreover, the broadening of peaks at 1130 and 1015 cm^{-1} was also observed that can be attributed to the formation of Si—O—Si[30] bonds in the G-HNTs sample. All these results clearly indicated that silane coupling agents were grafted on the HNTs surface, as evident from the TEM shown in Figure 1.

XRD Analysis

XRD patterns of G-HNTS powder, PHBV and PHBV/G-HNTs samples with different HNT loadings are shown in Figure 3. The XRD patterns of G-HNTs showed the basal peak at $2\theta = 12.1°$ corresponds to a (001) basal spacing of 0.73 nm. This confirms the nanosize of the HNTs as well as the tubular structure of them.[31,32] In PHBV/G-HNTs samples, the internal channel diffraction peak at (001 plane) was found to shift to lower angle indicating a layer expansion of the HNT tubes. From the results, it was also noticed that the interlayer distance of the basal plane increased from 0.73 to 0.743 nm (1 wt %), 0.747 nm (2 wt %) and 0.752 nm (3 wt %) in PHBV/G-HNTs samples. This increase in the interlayer spacing indicates that the PHBV may have been successfully intercalated inside the HNT layer. Also, it was noticed that the diffraction peak intensitys found in G-HNTs at $2\theta = 12.1$ and $2\theta = 19.98$ disappeared in PHBV/G-HNTs samples, indicating a high degreee of exfoliation of G-HNTs in PHBV resin. It is clearly evident from these results that the G-HNTs were homogeneously dispersed due to the strong interaction between the PHBV polymer and HNT, which has originated from the formation of strong covalent bonding between the carbonyl group of PHBV and amino functional groups of G-HNTs as shown in Figure 4.

SEM and FTIR Analysis of Jute Fiber

Figure 5 shows the SEM micrographs of UT, AT, and AST jute-fibers. The as-received UT fibers contain lignin, pectin, waxes, cellulose and hemicellulose in their structure. After alkali treatment, waxes, impurities and non-cellulosic substances were removed, resulting in separation of fibers [Figure 5(c)]. Also, rougher surface was obtained due to acetylation of jute fibers [Figure 5(d)].

The separation of jute fiber bundle with a rougher surface increased the effective area available for contact with the wet matrix.[33,34] Micrographs of AST fibers showed the presence of a silane grafting on the fiber surface evident from Figure 5(e,f).

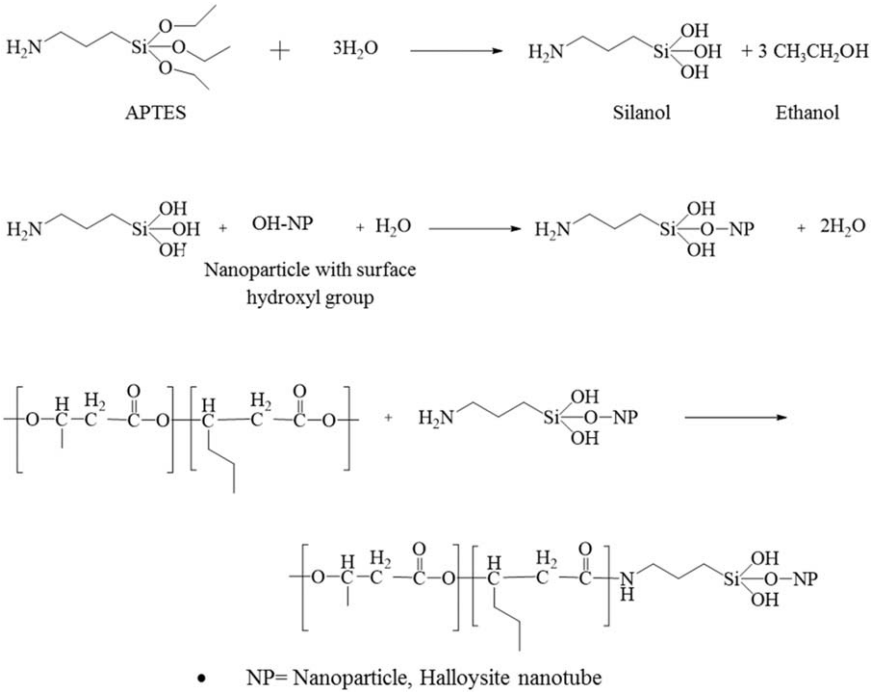

Figure 4. Reaction mechanism between silane grafted HNT and PHBV resin.

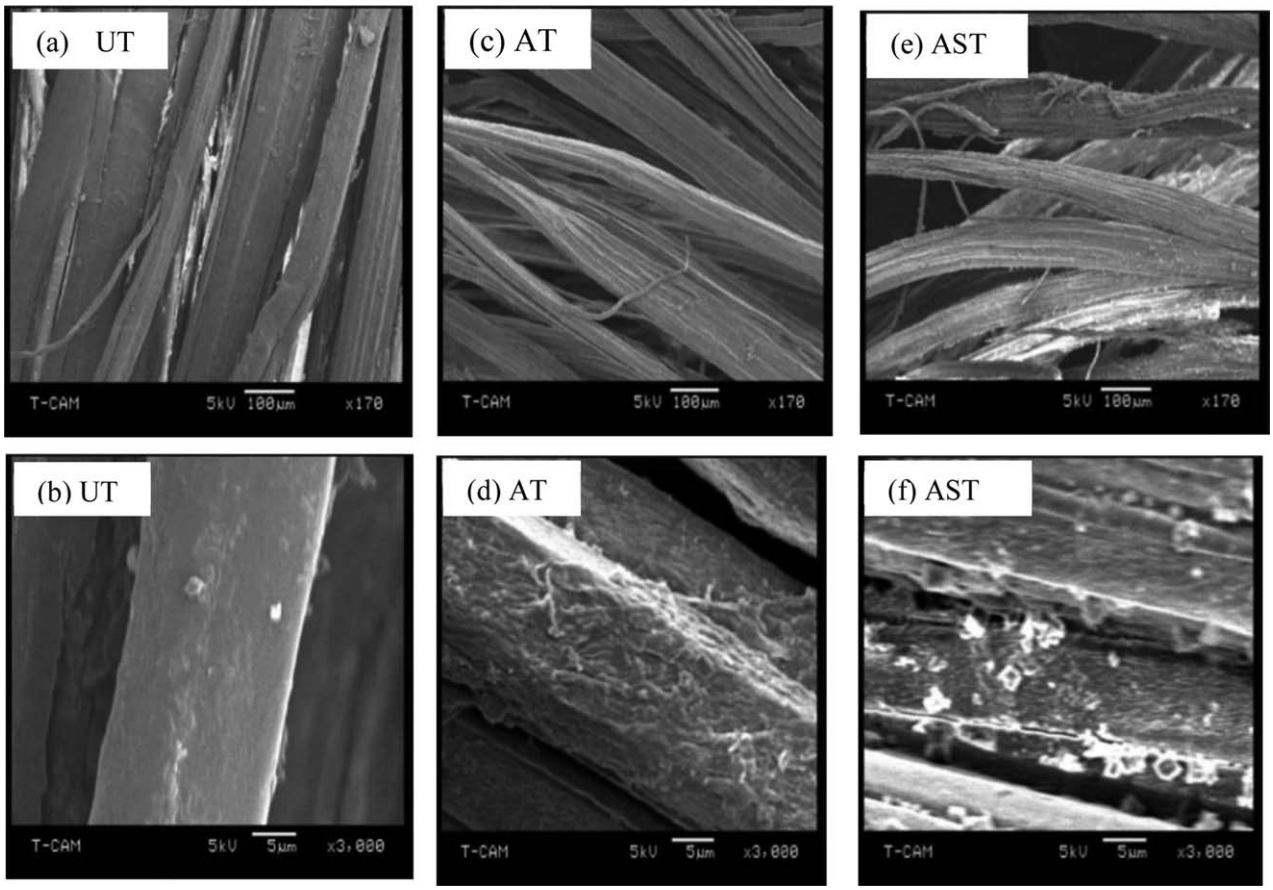

Figure 5. SEM micrographs of, (a,b) untreated (UT), (c,d) alkali treated (AT), and (e–f) alkali-silane treated (AST) jute fibers.

Figure 6 shows the FTIR spectra of UT, AT and AST jute fibers. In the range of 3200–3600 cm^{-1}, a broad absorption band was observed due to the stretching vibration of H-bonded —OH groups which was found common to all spectra. However, after the alkali treatment, this O—H stretching vibration was reduced. A strong peak for C—H bond observed near vibration band 2930 cm^{-1} [35] in UT fibers. This is due to the stretching of —CH and —CH_2 groups present in cellulose, hemicellulose, and pectin. The intensity of this vibration was reduced after the alkali treatment indicating the removal or minimization of hemicellulose and pectin content. Also, the wavenumber at 1730 cm^{-1} [36] in UT fibers represented the C═O stretching vibration of a carboxylic acid and ester present in the hemicelluloses. However, after the alkali treatment, this vibration peak was also reduced. The absorbance band at 1450 cm^{-1} and 1040 cm^{-1} responsible for -CH_3 asymmetric and —CH aromatic stretching in lignin was also reduced after alkali treatment, thus confirming the removal or minimization of lignin content in treated fibers.

The AST jute fiber FTIR spectra showed some additional absorption peaks at 1570 cm^{-1} and 1482 cm^{-1} which is due to the deformation modes of amino groups that are strongly hydrogen bonded with the hydroxyl groups of cellulose present in the fibers and silanol groups formed during hydrolysis of silane coupling agent. Thus, the FTIR spectra of AST fibers confirmed the minimization of hydrophilic content and successful grafting of silane agents on the fiber surface, matching well with the SEM images shown in Figure 5 (e,f).

Flexural Properties

Figure 7 shows the flexural results of UT and AST jute fiber-PHBV composites with and without G-HNTs. The flexural strength and modulus of AST samples were improved by 18.6%

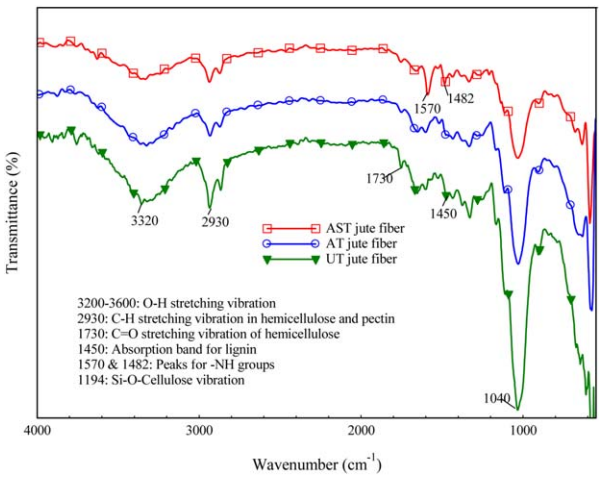

Figure 6. FTIR spectra of UT, AT, and ATS treated jute fibers. [Color figure can be viewed in the online issue, which is available at wileyonlinelibrary.com.]

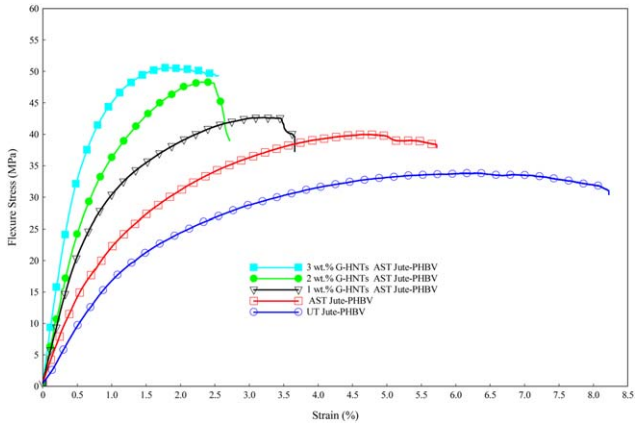

Figure 7. Flexural stress–strain curve of UT, AST, and AST with 1–3 wt % G-HNTs added jute-PHBV bio-nanocomposites. [Color figure can be viewed in the online issue, which is available at wileyonlinelibrary.com.]

and 19% in comparison with UT counterpart. The AST fibers may have formed a better adhesion with the polymer matrix due to removal of hydroxyl groups that provided more surface area for fiber wettability with PHBV matrix. In addition, after silane treatment, the functional groups of silane reacted with water forming silanol and alcohol.[38] The silanol then reacts with the hydroxyl group of the fibers forming a stable covalent bond. Further, when these fibers were combined with the PHBV polymer, the NH_2 of fiber reacts with the PHBV carbonyl functional groups as shown in Figure 8. As a result, the interfacial bonding between jute fiber and PHBV matrix may have increased leading to the increase in flexural strength and modulus of AST samples. However, G-HNTs added AST samples showed a linear increase in flexural strength and modulus with an increase of 25% and 35% at 1 wt %, 36% and 51% at wt %, and a maximum improvement of 49% and 63% at 3 wt % loading in comparison with UT samples. This additional improvement in flexural properties can be attributed to the addition of G-HNTs. The surface energy may have reduced providing uniform dispersion of HNTs in PHBV resin. As a result, the HNTs were well exfoliated in the PHBV polymer evident from XRD results (Figure 3) and provided more sites for their interaction. In addition, the G-HNTs contain a strong nucleophile amino functional group that has reacted with the carbonyl group of PHBV leading to a formation of a strong covalent bond, the reaction mechanism of which is shown in Figure 4. Chemically interlocked resin and HNTs structure lead to improved PHBV matrix strength and has improved the interfacial bonding between the jute fiber and PHBV matrix forming a three-way reaction, thus facilitating improved stress transfer between them. It can be seen from Figure 9 (c,d) that the 3 wt % G-HNTs samples offered high resistance to applied load prior to failure evident from intensive damage in the region where the load was applied and the frequent divergence of the crack path indicating improved matrix strength and fiber-matrix bonding. In contrast, less damage area in the region of loading and free crack propagation was observed in UT samples [Figure. 9 (a,b)] indicating weak interfacial bonding between fiber and matrix. Also, because of the strong interfacial bonding between G-HNTs and PHBV, the cracks that are formed upon loading may have stabilized by the nanotube bridging and stopped developing into a harmful crack.[39] However, the improved interfacial bonding between jute fiber and PHBV matrix lead to decrease in strain to failure in AST treated samples in comparison with UT samples. A further decrease in strain to failure was found when G-HNTs were incorporated in PHBV, which can be attributed to improved chemical interlocked structure that may have reduced the mobility of PHBV polymer chains (Figure 7).

Dynamic Mechanical Analysis (DMA)

Figure 10 and Table I shows the storage modulus, loss modulus and tan delta results of UT, AST with and without G-HNTs jute-PHBV samples with respect to temperature. It was observed that the storage modulus of samples was highest at room temperature and gradually decreased with increase in temperature. The AST samples showed an increase in the storage modulus of 14% in comparison with UT counterpart. Similar to flexure results, a linear increase in storage modulus was observed in G-HNTs added AST samples with a maximum increase of 31% at 3 wt % loading. However, the loss factor, tan δ, was found to decrease with the addition of HNTs with the lowest in 3 wt % G-HNTs loading samples in comparison with UT samples as shown in Figure 10. The tan δ provides the account of energy dissipated as heat during the dynamic testing.[40] Higher tan δ value in UT samples can be attributed to more energy dissipation at the interface between jute fiber and PHBV matrix indicating weak bonding. In contrast, the decrease in loss factor in G-HNTs samples can be attributed to a higher degree of crystallinity. Crystalline structures reduce the loss modulus giving rise to the storage modulus. Loss modulus is related to the molecular chain mobility of the polymer. The lower loss modulus in G-HNTs samples in comparison with UT samples evident from Table I can be attributed to the nanotubes and improved interfacial bonding between the HNTs, PHBV and fibers that may

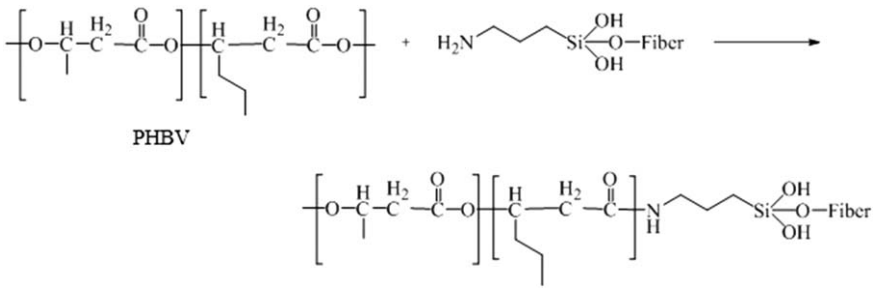

Figure 8. Reaction mechanism between APTES grafted jute fiber and PHBV matrix.

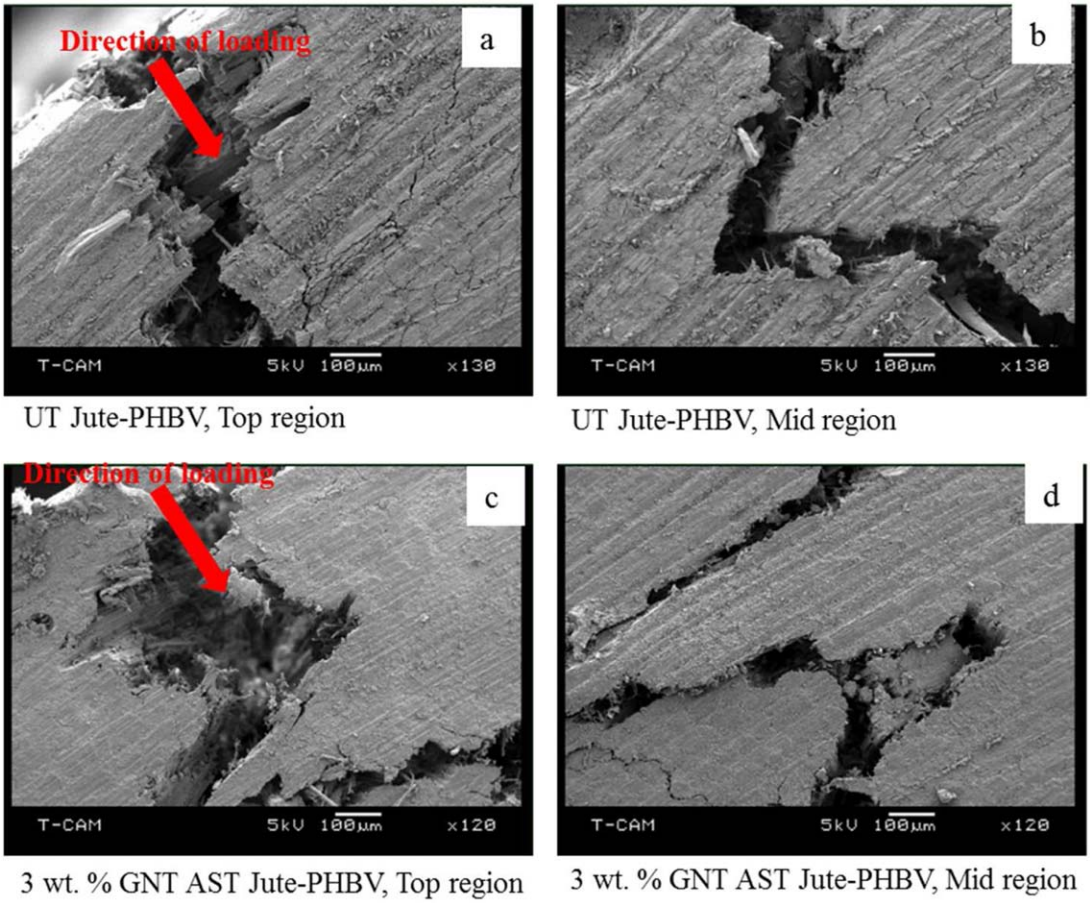

Figure 9. SEM images of fractured samples under flexural loading. [Color figure can be viewed in the online issue, which is available at wileyonlinelibrary.com.]

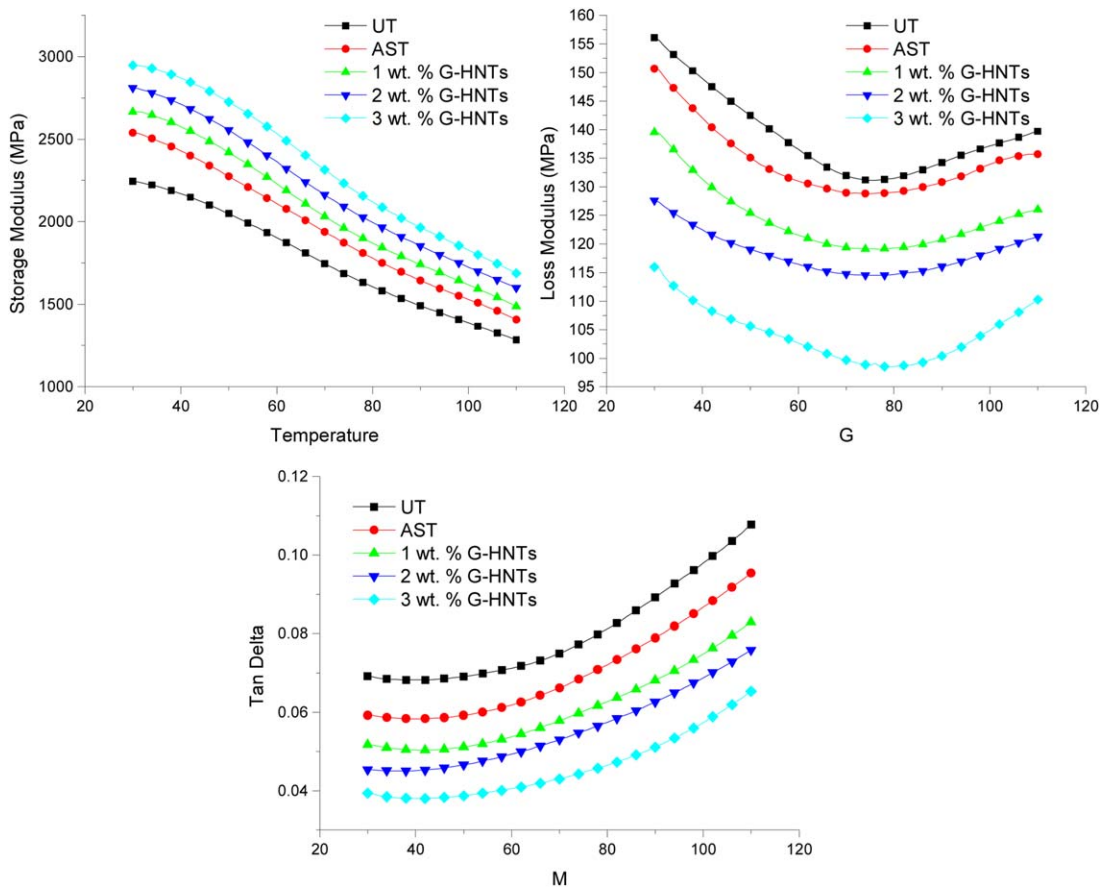

Figure 10. Storage modulus, loss modulus, and tan delta vs. temperature response of UT, AST, and AST with 1–3 wt % G-HNTs added jute-PHBV bio-nanocomposites. [Color figure can be viewed in the online issue, which is available at wileyonlinelibrary.com.]

Table I. DMA Data of UT, AST, and AST with 1–3 wt % G-HNTs Added Jute-PHBV Bio-Nanocomposites

Sample	Storage modulus (MPa) at 30 °C	% Change w.r.t to UT	Tan δ	Loss modulus (MPa) at 30 °C	% Change w.r.t to UT
1	2252 ± 88	X	0.07	155 ± 5.2	X
2	2570 ± 138	+14	0.06	151 ± 7.3	−3
3	2698 ± 122	+20	0.05	137.6 ± 6.6	−11
4	2810 ± 76	+25	0.05	126 ± 8.5	−19
5	2948 ± 102	+31	0.04	114 ± 5.2	−26

1-UT, 2-AST, 3-1 wt % G-HNTs AST, 4-2 wt % G-HNTs AST, and 5-3 wt % G-HNTs AST.

have imposed restriction on the expansion of the molecular chain in the amorphous region.

CONCLUSIONS

The alkali treatment caused defibrillation and made the fiber surface rough. FTIR results confirmed the decrease of hemicellulose, lignin and pectin content in addition to the presence of amino functional groups on the fiber surface after alkali treatment and surface modification with a silane coupling agent. TEM images showed an increase in HNTs diameter indicating the HNTs were grafted with amino groups, which was also confirmed from FTIR analysis. XRD results showed complete exfoliation of G-HNTs in PHBV and the intercalation of PHBV polymer in HNT layers. Maximum enhancement in flexural and thermo-mechanical properties was observed in 3 wt % G-HNTs AST jute-PHBV samples in comparison with untreated counterpart. It can be concluded from the findings that the properties of jute-PHBV biocomposites can be improved by following the traditional approach of alkali treatment and silane modification of fibers. The amino groups present on the surface of fibers formed strong covalent bond with the PHBV matrix leading to strong interfacial bonding and improved stress transfer between them. However, the most promising outcome of this study is the maximum enhancement in jute-PHBV composite properties using grafted HNTs. The grafting of HNTs with strong nucleophile amino functional groups that not only improved the dispersion providing more interaction sites with PHBV resin, but also formed a covalent bonding with the PHBV resin. Thus, this chemically interlocked resin and HNTs structure lead to improved PHBV biopolymer strength and stiffness. Also, because of the strong interfacial bonding between G-HNTs and PHBV, the cracks that are formed upon loading may have stabilized by the nanotube bridging and stopped developing into a harmful crack. Thus, it is shown that the much concern poor strength and stiffness of biocomposites can be successfully improved by reinforcing silane grafted HNTs. It will be interesting to investigate the flexure and DMA properties of jute-PHBV composites by further increasing the concentration of HNTs loading until an optimization or saturation limit is reached, which is out of scope of this work.

ACKNOWLEDGMENTS

The authors acknowledge the financial support of NSF-CREST Grant No. HRD-1137681, NSF HBCU-RIA Grant No. HRD-1409918 NSF-EPSCoR Grant No. EPS-1158862, and NSF-REU Grant No. DMR-1358998 for this research work.

REFERENCES

1. Saheb, D. N.; Jog, J. P. *Inc. Adv. Polym. Techn.* **1999**, *18*, 351.
2. Bos, H. L.; Müssig, J.; vandenOever, M. J. A. *Compos. Part A: Appl. Sci. Manuf.* **2006**, *37*, 1591.
3. Li, X.; Tabil, L. G.; Panigrahi, S. *J. Polym. Environ.* **2007**, *15*, 25.
4. Ouajai, S.; Hodzic, A.; Shanks, R. A. *J. Appl. Polym. Sci.* **2004**, *94*, 2456.
5. Zah, R.; Hischier, R.; Leão, A. L.; Braun, I. *J. Clean Prod.* **2007**, *15*, 1032.
6. Mishra, S.; Mohanty, A. K.; Drzal, L. T.; Misra, M.; Hinrichsen, G. *Macromol. Mater. Eng.* **2004**, *289*, 955.
7. Dweib, M. A.; Hu, B.; O'Donnell, A.; Shenton, H. W.; Wool, R. P. *Comp. Struct.* **2004**, *63*, 147.
8. Hong, C. K.; Hwang, I.; Kim, N.; Park, D. H.; Hwang, B. S.; Nah, C. J. *Ind. Eng. Chem.* **2008**, *14*, 71.
9. Abdelmouleh, M.; Boufi, S.; Belgacem, M. N.; Duarte, A. P.; BenSalah, A.; Gandini, A. *Int. J. Adhes. Adhes.* **2004**, *24*, 43.
10. Ray, D.; Sarkar, B. K.; Das, S.; Rana, A. K. *Compos. Sci. Technol.* **2002**, *62*, 911.
11. Mohanty, A.; Khan, M.; Hinrichsen, G. *Comp. Part A: Appl. Sci. Manufact.* **2000**, *60*, 1115.
12. Sain, M. M.; Kokta, B. V. *J. Reinforc. Plast. Comp.* **1994**, *13*, 54.
13. Gassan, J.; Bledzki, A. K. *Comp. Part A: Appl. Sci. Manufact.* **1997**, *28*, 1001.
14. Doan, T. T. L.; Gao, S. L.; Mäder, E. *Compos. Sci. Technol.* **2006**, *6*, 952.
15. Herrera-Franco, P. J.; Valadez-González, A. *Comp. Part A: Appl. Sci. Manufact.* **2004**, *35*,339.
16. Bengtsson, M.; Oksman, K. *Compos. Part A: Appl. Sci. Manufact.* **2006**, *37*, 752.
17. Khan, M. A.; Hassan, M. M. *J. Appl. Polym. Sci.* **2006**, *100*, 4142.
18. Van de Weyenberg, I.; Ivens, J. D.; Coster, A.; Kino, B.; Baetens, E.; Verpoest, I. *Compos. Sci. Technol.* **2003**, *63*, 1241.
19. Zini, E.; Focarete, M. L.; Noda, I.; Scandola, M. *Compos. Sci. Technol.* **2007**, *67*, 2085.

20. Agrawal, R.; Saxena, N.; Sharma, K.; Thomas, S.; Sreekala, M. *Mater. Sci. Eng.: A* **2000**, *277*, 77.
21. Huda, M. S.; Drzal, L. T.; Mohanty, A. K.; Misra, M. *Compos. Sci. Technol.* **2008**, *68*, 424.
22. Yuan, P.; Southon, P. D.; Liu, Z.; Green, M. E. R.; Hook, J. M.; Antill, S. J.; Kepert, C. J. *J. Phys. Chem. C* **2008**, *112*, 15742.
23. Kamble, R.; Ghag, M.; Gaikawad, S.; Panda, B. K. *J. Adv. Sci. Res. J. Adv. Sci. Res.* **2012**, *3*, 25.
24. Du, M.; Guo, B.; Lei, Y.; Liu, M.; Jia, D. *Polymer (Guildf)* **2008**, *49*, 4871.
25. Ismail, H.; Shaari, S. M. *Polym. Test.* **2010**, *29*, 872.
26. Soheilmoghaddam, M.; Wahit, M. U.; Mahmoudian, S.; Hanid, N. A. *Mater. Chem. Phys.* **2013**, *141*, 936.
27. Prashantha, K.; Lacrampe, M. F.; Krawczak, P. *Exp. Polym. Lett.* **2011**, *5*, 295.
28. Zhao, M.; Liu, P. *J. Therm. Anal. Calorim.* **2008**, *94*, 103.
29. Pal, P.; Kundu, M. K.; Malas, A.; Das, C. K. *J. Appl. Polym. Sci.* **2014**, *131*, DOI: 10.1002/app.39587.
30. Carli, L. N.; Daitx, T. S.; Soares, G. V.; Crespo, J. S.; Mauler, R. S. *Appl. Clay Sci.* **2014**, *87*, 311.
31. Carli, L. N.; Crespo, J. S.; Mauler, R. S. *Compos. Part A: Appl. Sci. Manuf.* **2011**, *42*, 1601.
32. Chen, G. X.; Hao, G. J.; Guo, T. Y.; Song, M. D.; Zhang, B. H. *J. Appl. Polym. Sci.* **2004**, *93*, 655.
33. Pothan, L. A.; Thomas, S.; Groeninckx, G. *Compos. Part A: Appl. Sci. Manuf.* **2006**, *37*, 1260.
34. Razera, I. A. T.; Frollini, E. *J. Appl. Polym. Sci.* **2004**, *91*, 1077.
35. Zhou, F.; Cheng, G.; Jiang, B. *Appl. Surf. Sci.* **2014**, *292*, 806.
36. Haque, M. M.; Hasan, M.; Islam, M. S.; Ali, M. E. *Bioresour. Technol.* **2009**.
37. John, M. J.; Francis, B.; Varughese, K. T.; Thomas, S. *Compos. Part A: Appl. Sci. Manuf.* **2008**, *39*, 352.
38. Ye, Y.; Chen, H.; Wu, J.; Ye, L. *Polymer* **2007**, *48*, 6426. (Guildf)
39. Group, F.; Avenue, M.; Square, P.; Park, M.; Ox, O. Library of Congress Cataloging-in-Publication Data Visit the Taylor & Francis Web site **2005**.